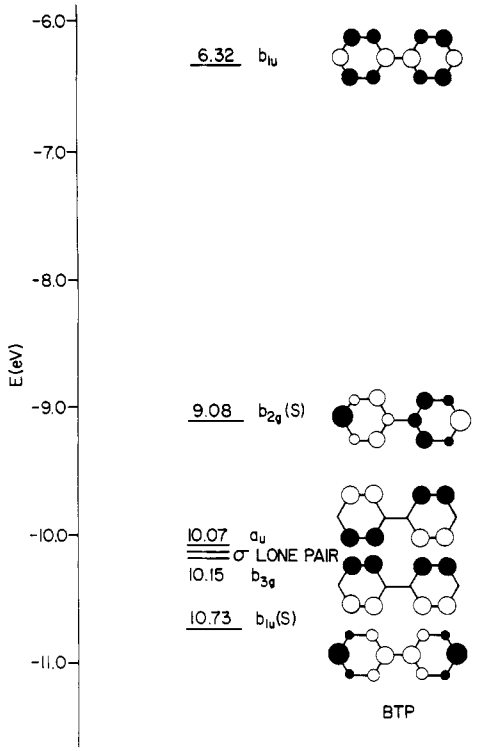

Figure 9. Results of CNDO/S3 calculation for BTP.

spectra of $TTF(CN)_4$ shows a single level at 11.0 eV followed by a doubly degenerate level at 11.4 eV and suggests that the ordering of the lone pairs is b_{1g} (σ), a_1 (π), b_{3g} (π) as given by the CNDO/S3 calculations.

The UPS spectra and CNDO/S3 calculations for TTF and TPDT are noteworthy in that the sequence of ionization potentials for TTF (6.81, 8.71, 9.75, 10.17, 10.49, and 11.08 eV) is within experimental error virtually identical with that for TPDT (6.68, 8.77, 9.92, 9.92, 10.40, and 11.00 eV). This indicates that within the Koopmans' theorem limit, the ground-state orbital properties of the two molecules are very similar. The donor–acceptor complexes formed with TCNQ in the solid state by these two species, however, are completely different, with TTF forming a metallic salt while TPDT forms semiconducting salts. The first ionization potential, redox potential, and ground-state valence structure are clearly necessary conditions for electron transfer in donor–acceptor interactions with acceptors, such as TCNQ.[8b] They are also necessary, but clearly not sufficient, conditions in determining solid-state properties of the resultant ion–radical solids.[8b] Here other factors (e.g., kinetic control of solid-phase formation,[8c,34] solid-state structure and packing,[10b] charge stabilization) are at least equally as important.

The CNDO/S3 calculations for BTP are interesting in that the first IP of this species is predicted to occur at 6.3 eV, significantly lower than that of TPDT and TTF. While the UPS of a BTP derivative has not been measured, cyclic voltammetry shows $E_{1/2}$ for BTP at 0.20 V vs SCE.[35] This should be compared to the $E_{1/2}$ values for TTF[3a,8b] and TPDT: 0.33 and 0.28 V, respectively. BTP is a stronger reducing agent as predicted by CNDO/S3 calculations, which are summarized in Figure 9. While there is a broad correlation between gas-phase IP and $E_{1/2}$, the limitations of such correlations have been discussed by the present authors.[8b,d,23a]

Acknowledgment. We thank T. J. Holmes and D. E. Warner for technical assistance and M. J. Downey for furnishing X-ray powder diffraction data.

Supplementary Material Available: Tables listing least-squares planes (1 page) and observed and calculated structure factors (8 pages). Ordering information is given on any current masthead page.

(34) Sandman, D. J. *J. Am. Chem. Soc.* **1978**, *100*, 5230.
(35) Hünig, S.; Garner, B. J.; Ruider, G.; Schenk, W. *Justus Liebigs Ann. Chem.* **1973**, 1036.

X-Ray Photoelectron Spectroscopic Studies of Carbon Fiber Surfaces. 10. Valence-Band Studies Interpreted by X-α Calculations and the Differences between Poly(acrylonitrile)- and Pitch-Based Fibers

Yaoming Xie and Peter M. A. Sherwood*

Department of Chemistry, Willard Hall, Kansas State University, Manhattan, Kansas 66506

Received March 7, 1989

X-ray photoelectron spectroscopy has been used to monitor the surface chemistry of untreated carbon fibers based on poly(acrylonitrile) and pitch. Differences were found in the core and valence-band region indicating a highly graphitic and an almost unoxidized nature for pitch-based fibers. The valence-band region of the most graphitic fiber compares well with a spectrum obtained from orbital energies and atomic contributions from an X-α calculation on coronene ($C_{24}H_{12}$).

Introduction

Carbon fibers are widely used in composite materials, especially in the aircraft industry, where the high stiffness-to-weight ratio of such composites is important. Commercially available carbon fibers are obtained either from heat treatments of polymeric materials such as poly(acrylonitrile) (PAN) or from carbon sources such as pitch from petroleum or coal tar.

The surface structure of carbon fibers is an important factor in the effective adhesion between the fiber and the composite matrix. We have carried out a series of studies[1-9] of the surface of carbon fibers based upon PAN using

(1) Proctor, A.; Sherwood, P. M. A. *J. Electron Spectrosc.* **1982**, *27*, 39.
(2) Proctor, A.; Sherwood, P. M. A. *Carbon* **1983**, *21*, 53.

0897-4756/89/2801-0427$01.50/0

core X-ray photoelectron spectroscopy (XPS or ESCA). We have reviewed other XPS work in this area in a previous publication.[9] In this paper we consider the differences in the surface chemistry of fibers based upon PAN and those based upon pitch. In particular we report studies of the valence band of the carbon fibers, with the spectra interpreted by an X-α calculation on coronene which is used as a model for the graphite lattice. We show that the valence band can be well interpreted by the X-α calculation and that the valence band is very sensitive to changes in carbon fiber surface chemistry.

Experimental Section

Three types of carbon fibers were used in this work. Sample a was an untreated PAN-based type II (high-strength) fiber (from the same source as that used in our previous studies[1-9]), which was washed with triply distilled water, dried at 120 °C for 24 h, and then stored in a glass container for 16 months. Sample b was an untreated PAN-based type II Hercules AU4 carbon fiber, and sample c was an untreated pitch-based Amoco P55X carbon fiber.

The X-ray photoelectron (XPS or ESCA) spectra were collected on an AEI (Kratos) ES200B X-ray photoelectron spectrometer with a base pressure of about 10^{-9} Torr. The XPS spectrometer was operated in the constant retarding ratio (FRR) mode (ratio 1:23) using Mg $K\alpha_{1,2}$ X-ray radiation (240 W). Analyzer resolution was of the same order as the X-ray line width (0.8 eV). Typical data collection times were as follows: C(1s), 1 h; O(1s), 10 h; N(1s), 5–40 h; valence band, 16 h. No sample decomposition was observed during data collection. The spectrometer energy scale was calibrated by using copper[10] and using the separation (233 eV) between photoelectron peaks generated by Mg and Al $K\alpha_{1,2}$ X-rays.

X-ray powder diffraction studies were carried out by using a Scintag θ–θ instrument.

A bundle of carbon fibers was cut to a length of 3.0 cm, with both ends tied with a piece of narrow aluminum foil. One of the ends was then mounted in a metal sample holder. After insertion into the XPS spectrometer chamber, the sample was connected to the system ground by the metal sample holder. The position of the sample holder was adjusted so that no photoelectrons were seen from the sample holder or the aluminum foil.

The curve fitting of the XPS spectra was carried out by using a nonlinear least-squares curve-fitting program with a Gaussian/Lorentzian product function.[11,12] The Gaussian/Lorentzian mix was taken as 0.5, except for the "graphitic" carbon peak, which was taken as 0.84 with an exponential tail. The C(1s) binding energy of the graphitic peak was taken as 284.6 eV for calibration purposes.

Results and Discussion

The overall XPS spectra for all three samples are shown in Figure 1. These samples showed an intense C(1s) peak, a weak C(KLL) Auger peak, and a weak O(1s) peak (especially weak for the pitch-based sample that it is hardly visible in Figure 1). The N(1s) peak was of very low intensity in all cases and could not really be detected for the pitch based sample.

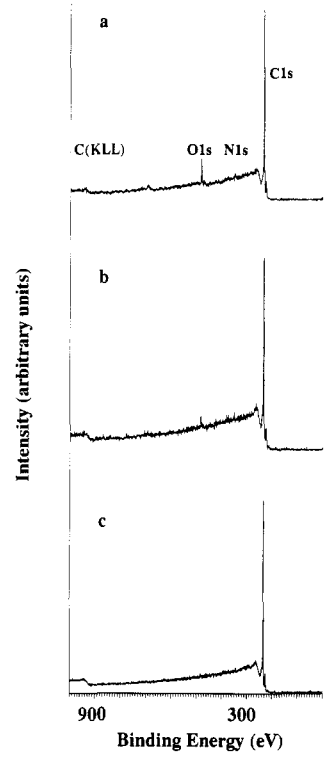

Figure 1. Overall spectra of various untreated carbon fiber samples: (a) type II PAN-based fiber; (b) AU4 PAN-based fiber; (c) P55X pitch-based fiber.

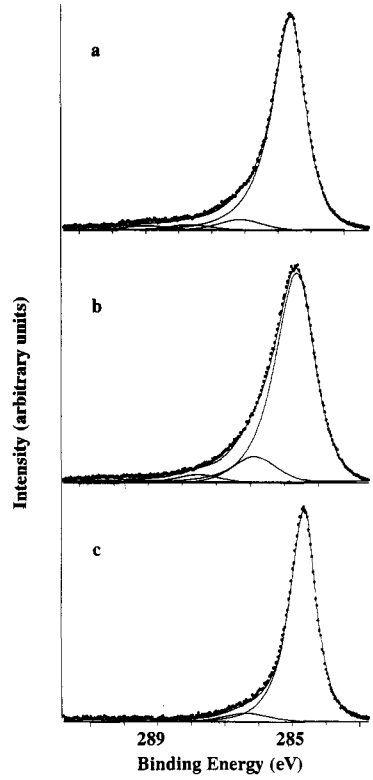

Figure 2. C(1s) spectra of various untreated carbon fiber samples: (a) type II PAN-based fiber; (b) AU4 PAN-based fiber; (c) P55X pitch-based fiber.

C(1s) Region. Figure 2 shows the curve fitted C(1s) spectra. It is known that certain types of functional groups exist on carbon fiber surfaces, even fibers that are not sized or surface treated. Each functional group gives rise to a

(3) Proctor, A.; Sherwood, P. M. A. *Surf. Interface Anal.* **1982**, *4*, 212.
(4) Kozlowski, C.; Sherwood, P. M. A. *J. Chem. Soc., Faraday Trans. 1* **1984**, *80*, 2099.
(5) Kozlowski, C.; Sherwood, P. M. A. *J. Chem. Soc., Faraday Trans. 1* **1985**, *81*, 2745.
(6) Harvey, J.; Kozlowski, C.; Sherwood, P. M. A. *J. Mater. Sci.* **1987**, *22*, 1585.
(7) Kozlowski, C.; Sherwood, P. M. A. *Carbon*, **1986**, *24*, 357.
(8) Kozlowski, C.; Sherwood, P. M. A. *Carbon*, **1987**, *25*, 751.
(9) Xie, Y.; Sherwood, P. M. A. *Appl. Spectrosc.*, in press.
(10) Annual Book of ASTM Standards, Vol. 03.06, published in *Surf. Interface Anal.* **1988**, *11*, 112.
(11) Sherwood, P. M. A. *Practical Surface Analysis by Auger and Photoelectron Spectroscopy*; Briggs, D., Seah, M. P., Eds.; Wiley: London, 1983; Appendix 3.
(12) Ansell, R. O.; Dickinson, T.; Povey, A. F.; Sherwood, P. M. A. *J. Electroanal. Chem.* **1979**, *98*, 79.

Table I. C(1s) Peaks and Relative Peak Areas

sample	C(1s) peaks in different states BE, eV (area, %) oxide 4	oxide 3	oxide 2	oxide 1	main peak	oxides area (1 + 2 + 3 + 4), %
a	290.6 (0.5)	289.0 (3.3)	287.7 (2.5)	286.1 (5.8)	284.6 (87.9)	12.1
b	290.5 (0.7)	289.0 (1.8)	287.5 (3.2)	285.9 (11.9)	284.6 (82.4)	17.6
c	290.8 (0.8)	290.3 (0.3)	287.8 (0.8)	286.3 (6.6)	284.6 (91.6)	8.4

Table II. O(1s) Peaks, Relative Peak Areas, and Atomic Ratios

sample	O(1s) peaks in different states BE, eV (area, %) peak 1	peak 2	peak 3	O(1s)/C(1s) peak area ratio, %	at. amt ratio O/C	N/C	(O + N)/C
a	536.3 (1.2)	533.5 (69.5)	532.0 (29.4)	9.38	4.62	1.16	5.78
b	535.9 (3.3)	533.2 (79.8)	531.8 (16.9)	5.59	2.76	3.20	5.96
c	536.1 (9.5)	533.1 (79.2)	531.5 (11.3)	3.48	1.72	0	1.72

Table III. N(1s) Peaks and Relative Peak Areas

sample	N(1s) peaks in different states BE, eV (area, %) peak 1	peak 2	peak 3	peak 4	peak 5	N(1s)/C(1s) peak area ratio, %
a	404.9 (9.4)	403.0 (21.9)	401.4 (45.7)	400.0 (14.3)	398.9 (8.7)	1.79
b	405.3 (7.5)	402.6 (14.9)	401.1 (58.8)	399.3 (5.4)	398.3 (13.4)	4.95
c[a]						0

[a] No N(1s) signal could be detected.

Chart I

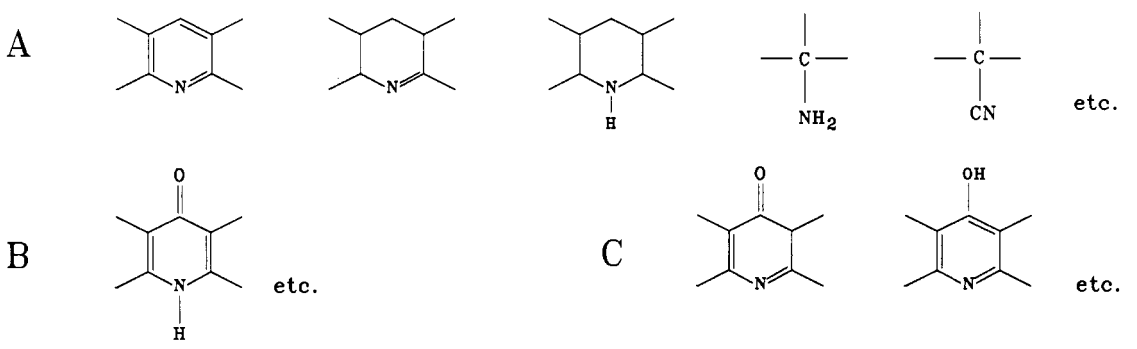

signal in the XPS spectrum with a particular range of binding energies.[1-9,13,14] In this work, the C(1s) spectra show one main "graphitic" peak at 284.6 eV and four "oxide" peaks. The four types of oxide called oxide 1, 2, 3, and 4 were shifted by 1.5, 3.1, 4.5, and 6.0 eV from the graphitic peak, respectively. Oxide 1 is assigned to the carbon atom in alcohol (C–OH) or ether (C–O–C) groups. The C(1s) signal from C=N type groups also falls into this range. Oxide 2 corresponds to the C atom in carbonyl (C=O) type groups. Oxide 3 is the C(1s) peak of carboxyl (COOH) or ester (COOR) type groups. Oxide 4 is probably $-CO_3^-$ type groups, and the $\pi-\pi^*$ shake up satellite is also in this range. The conducting nature of graphitic lattice will also give rise to a plasmon feature of about 6.9-eV shift from the graphitic peak, but it is not included in the range of Figure 2. Some of these groups were confirmed by FTIR.[4]

Table I gives the peak positions and peak area percentages for C(1s) spectra. Sample a was stored after washing and drying for a longer period (16 months) than that reported for our earlier[9] work (3 months). The longer storage period leads to more oxidation. Sample b was the most highly oxidized sample (showing considerable amounts of C–N, C–OC, C–OH, and C=O groups), and sample c was the least oxidized sample.

The most significant difference among these samples is the low level of oxidation and the very narrow "graphitic" peak (see Figure 2) of the pitch-based sample. The fwhm of the graphitic peak of sample c is only 0.79 eV, while those of samples a and b are 1.01 and 1.20 eV, respectively. The fwhms of all the oxide peaks of samples a, b, and c are about the same (1.55 eV). Narrow C(1s) "graphitic" peaks have been previously reported for pitch-based fibers.[15]

O(1s) Region. Figure 3 shows the O(1s) region spectra fitted to three peaks. Peak 1 (ca. 536.1 eV) is of low intensity, and it is probably due to the adsorbed water and some chemisorbed oxygen. Peak 2 (ca. 533.3 eV) and peak 3 (ca. 531.8 eV) are the O(1s) signals from C–OH and C=O (or/and C–O–C) groups, respectively. Table II gives the binding energy and percentage areas of each O(1s) peak.

Peak 3 is relatively more intense in sample a than in the other samples. The long storage time for this sample showed an increase in C=O and C–O–C groups on the surface compared with samples stored for a shorter period.[9] The greatest amount of peak 2 was found for sample b. Table II also lists the ratio of the O(1s) peak area to the total C(1s) peak area and the O/C and O/N atomic ratio obtained by using Scofield's cross sections[16] and the in-

(13) Da, Y.; Wang, D.; Sun, M. *Compos. Scien. Technol.* **1987**, *30*, 119.
(14) Takahagi, T.; Shimada, I.; Fukuhara, M.; Morita, K.; Ishitani, A. *J. Polym. Scien., Polym. Chem. Ed.* **1986**, *24*, 3101.
(15) Santiago, F.; Mansour, A. N.; Lee, R. N. *Surf. Interface Anal.* **1987**, *10*, 17.

Table IV. Component O(1s) and N(1s) Peak Areas Expressed as a Ratio of the Total C(1s) Peak Area

	area, %							
	O(1s)/Cl(1s) (total)			N(1s)/C(1s) (total)				
sample	peak 1	peak 2	peak 3	peak 1	peak 2	peak 3	peak 4	peak 5
a	0.11	6.52	2.76	0.17	0.39	0.82	0.26	0.16
b	0.19	4.46	0.94	0.37	0.74	2.91	0.27	0.66
c	0.33	0.76	0.39	*a*	*a*	*a*	*a*	*a*

[a] No N(1s) signal is detected.

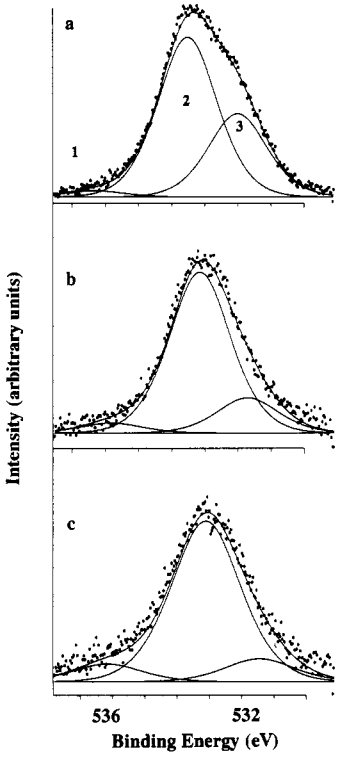

Figure 3. O(1s) spectra of various untreated carbon fiber samples: (a) type II PAN-based fiber; (b) AU4 PAN-based fiber; (c) P55X pitch-based fiber.

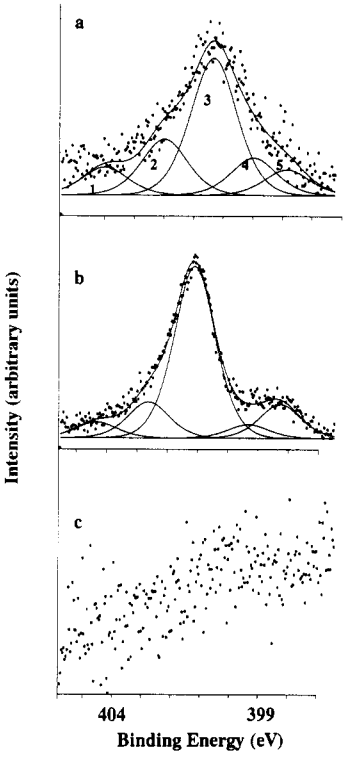

Figure 4. N(1s) spectra of various untreated carbon fiber samples: (a) type II PAN-based fiber; (b) AU4 PAN-based fiber; (c) P55X pitch-based fiber. The spectra are shown with different intensity scales, the scale being chosen to represent the difference between the maximum and minimum points in the data.

strument transmission function assuming a homogeneous sample.

N(1s) Region. N(1s) signal from carbon fiber surfaces is usually much weaker than C(1s) or O(1s) signals. Figure 4 shows the N(1s) Spectra of samples a, b, and c. Sample c, the pitch-based P55X fiber, shows no appreciable N(1s) signal. Sample b has the highest N(1s) signal level, while sample a has a weak but clearly shaped N(1s) peak.

The curve fitting of N(1s) spectra was carried out by using the approach discussed previously[9] where the best fit was obtained by using five peaks. In this approach peak 5 is assigned to the nitrogen in the groups of set A in Chart I, peak 4 to the nitrogen in set B, and peak 3 to the nitrogen in set C. Peaks 1 and 2 are probably shake-up satellites from the groups in sets A and B. There may also be some contribution from chemisorbed nitrogen. Table III shows the N(1s) peak positions and peak areas.

Comparison of C(1s) and N(1s) Spectra. Table IV shows the area ratios for the different XPS core regions. These ratios give consistent results since the bulk sensitivity follows the order C(1s) > N(1s) > O(1s) as discussed earlier.[9]

It can be seen that sample a has the highest and sample c the lowest oxygen functionality. Sample b has the highest nitrogen functionality, and sample c has hardly any detectable nitrogen functionality.

The pitch-based fiber has a narrower C(1s) peak (close to the natural width of the Mg X-rays used) than either of the PAN based fibers. This is partly due to the more complete graphitic structure (see the valence-band results discussed below) of the pitch-based fiber. We find that the C(1s) peak can be considerably broadened if the lattice is disordered by methods such as argon ion etching. Another cause for the narrower line width is the lack of nitrogen, removing the possibility of chemically shifted C–N groups which can be found as close as about 0.7 eV from the main "graphitic" peak.

Valence Band Studies: Model Calculations. The valence-band XPS spectra of various carbon materials, such as diamond, graphite, and glassy carbon have been well studied, e.g., ref 17–19, although there has been little work reported on the valence band of carbon fibers. We have recorded the X-ray diffraction pattern of all three fibers and compared it with that of graphite. We will discuss these results in more detail in a later publication,[20] but it should be pointed out here that the diffraction

(16) Scofield, J. H. *J. Electron Spectrosc.* **1976**, *8*, 129.

(17) Cavell, R. G.; Kowalczyk, S. P.; Ley, L.; Pollak, R. A.; Mills, B.; Shirley, D. A.; Perry, W. *Phys. Rev. B.* **1973**, *7*, 5313.

(18) McFeely, F. R.; Kowlaczyk, S. P.; Ley, L.; Cavell, R. G.; Pollak, R. A.; Shirley, D. A. *Phys. Rev. B* **1974**, *9*, 5268.

(19) Evans, S.; Riley, C. E. *J. Chem. Soc., Faraday Trans. 2* **1986**, *82*, 541.

(20) Xie, Y.; Sherwood, P. M. A., to be published.

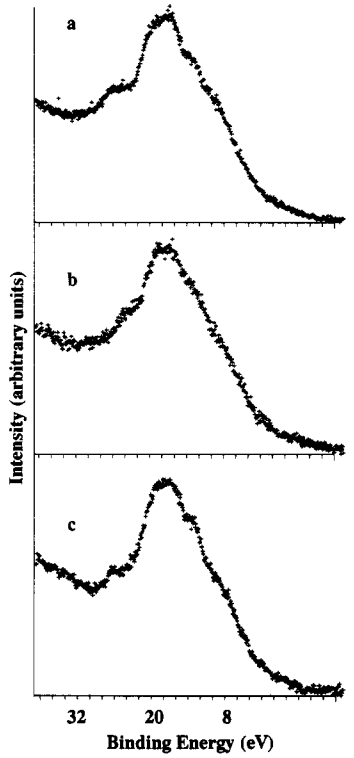

Figure 5. Valence-band spectra of various untreated carbon fiber samples: (a) type II PAN-based fiber; (b) AU4 PAN-based fiber; (c) P55X pitch-based fiber.

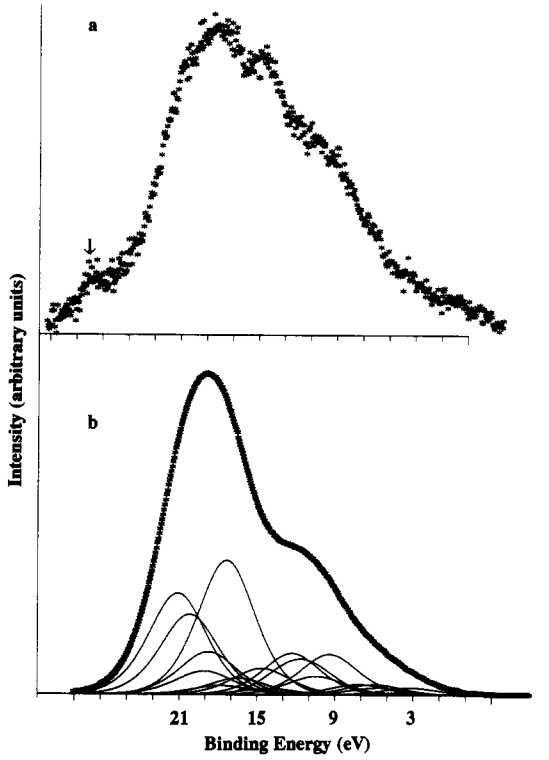

Figure 6. Valence-band spectrum of P55X pitched-based fiber compared with the spectrum predicted from an X-α calculation on coronene. The predicted spectrum is based upon the central C_6 ring in coronene.

pattern shows that the fibers have lines in the same position as graphite, with generally broader line widths. The pitch-based fiber sample has line widths only slightly broader than graphite. We thus conclude that the fibers studied are significantly graphitic (especially the pitch-based fiber), indicating that the valence-band spectra can be usefully interpreted using a graphitic model.

Figure 5 shows the valence band spectra of sample a, b, and c. It is noted that all three samples each has a similar valence band structure that resembles the graphite valence-band spectra.[18] The valence-band spectra of graphite have been compared with that of graphite valence-band studies.[18] In this work we have carried out an X-α calculation on the coronene molecule $C_{24}H_{12}$ with all the carbon–carbon distances set equal to those in graphite. The actual coronene molecule has some slight differences in the C–C distances and some distortion out of the plane. For our purposes the idealized D_{6h} molecule with graphite C–C distances seemed an appropriate model for graphite. We chose a molecular cluster calculation to model the graphite structure since we plan to carry out further cluster calculations on a coronene model with added functional groups to model-functionalized carbon fiber valence bands.

We have found that X-α calculations can be usefully applied to planar molecules such as benzene and coronene, even though the "muffin-tin" approach of the X-α method is used. We will discuss such calculations in another publication, which will also include full details of the coronene calculation.[21]

Figure 6 shows the spectrum of coronene from the X-α data. The energy scale has been shifted to correspond to the spectrum of the graphitic-like pitch-based fiber (also shown after removal of a nonlinear background[22] in Figure 6 for comparison). The details and features of the calculation are given in Table V. Transition-state calculations

Table V. Parameters Used and Features of the X-α Calculations

α values: carbon, 0.759 28; hydrogen, 0.776 54; outer sphere 0.767 91; inner sphere, 0.767 91
max l value: outer, 4; carbon, 2; hydrogen, 0
cluster: $C_{24}H_{12}$
symmetry: D_{6h}
C–C bond lengths: 1.420 Å
carbon sphere radius: 1.550 Å (central ring); 1.555 Å (closest C atoms to central ring); 1.595 Å (outer carbon atoms)
hydrogen sphere radius: 0.708 Å
outer-sphere radius: 5.169 Å
virial ratio ($-2T/V$): 1.024 014
convergence: when the difference in potentials at the beginning and end of the iteration were less than 10^{-5} of the potential at the start of the iteration; this gives energy levels that differed by less than 10^{-6} Ry between the last two iterations
core electrons: "thawed" so that they retained atomic character while being fully included in the iterative process; C(1s) electrons were treated as core electrons

were not attempted for coronene due to the large numbers of levels involved and the similarity between the relative transition-state and groung-state values for benzene[21] (which suggests that a coronene set of transition-state calculations might not give much difference from the ground-state data). The coronene result gives much the same prediction of the valence band features as the previously published graphite band structures, e.g. ref 23. In particular the most intense feature is due to C(2s) features, with C(2p) σ and then C(2p) π features to increasingly lower binding energy. The calculated spectrum was obtained by weighting the atomic contributions to the molecular orbitals with the Scofield cross sections.[16] The component energy levels were made up of equal-width Gaussian/Lorentzian product functions with a 50% mix (the same function used for fitting the spectra). Only data

(21) Edgar, C.; Sherwood, P. M. A., to be published.
(22) Proctor, A.; Sherwood, P. M. A. *Anal. Chem.* **1982**, *54*, 13.
(23) Painter, G. S.; Ellis, D. E. *Phys. Rev. B* **1970**, *1*, 4747.

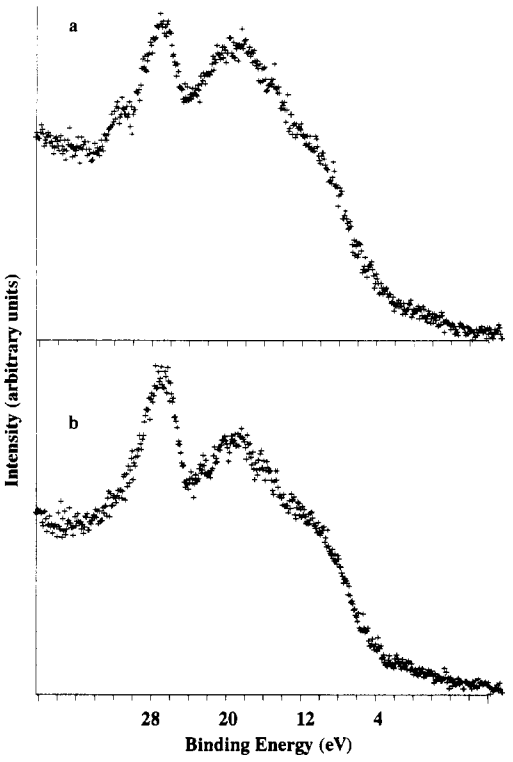

Figure 7. Valence-band spectra of commercially treated PAN-based fiber samples. Spectra a and b are for two different types of sample treatment.

for the central C_6 ring was used, as this ring is completely surrounded by other C_6 rings as in graphite. Variation in the width of levels might change some spectral features, but there is no direct justification for doing this. Overall the agreement with the pitch-based fiber and with previously published graphite spectra[18] is good. There is a feature to higher binding energy on the fiber spectrum that might be due to some oxygen 2p intensity, though it could equally be a true carbon 2s feature (the calculated spectrum has a peak at this energy, though the chosen widths do not give rise to the small shoulder). The feature at greatest binding energy in the fiber spectrum (marked by an arrow) is absent from the calculated spectrum and corresponds to oxygen 2s intensity. Figure 5 show that this feature is more prominent in the PAN-based fibers.

It is also interesting to note that this O(2s) feature is at a different position and shows different features in the two PAN spectra. In particular the spectrum of the PAN samples (especially of sample b, which has the largest amount of surface nitrogen) will also include some N(2s) intensity (the N(2s) features would be expected to lie between the C(2s) and O(2s) regions) which will complicate the spectrum. There will also be some O(2p) and N(2p) features, but the much lower cross section for these 2p electrons will greatly reduce their effect on the observed spectrum.

Figure 7 shows the valence band of some treated PAN fibers. The details of the treatment are confidential, but it can be seen that treatment causes a substantial increase in the O(2s) intentisty and that there is a clear structure on the O(2s) part of the spectrum. We have found in other systems[24] that the O(2s) region of the spectrum shows a greater sensitivity to chemical change than does the O(1s) region. This is due to the partial involvement in bonding for the O(2s) region. In our calculations on other systems[24] we find that the O(2s) features can be accurately predicted by X-α calculations, and we plan to use X-α calculations of oxidized coronene-based compounds to predict the valence-band spectrum of oxidized carbon fibers. What is clear is that the O(2s) features promise to be an important probe of carbon fiber surface functionality.

Conclusions

Carbon fibers based on pitch are clearly more graphitic and have a lower level of surface functionality than those based on PAN. The valence-band region of carbon fiber spectra can be reasonably interpreted by X-α cluster calculations, and the valence-band region promises to be a useful probe of subtle differences in surface functionality. In particular the oxygen 2s part of the valence band promises to be more sensitive to changes in oxygen functionality than the oxygen 1s region.

Acknowledgment. We are grateful to the Fibers Department of the Du Pont Company for supporting this work and to the Department of Defense for providing funding for the X-ray diffraction equipment.

Registry No. PAN, 25014-41-9; Nafion 117, 66796-30-3; Nafion NE111, 119823-05-1.

(24) Welsh, I. D.; Sherwood, P. M. A. *Phys. Rev. B*, submitted for publication.